Lawrence Berkeley National Laboratory
Energy Storage & Distributed Resources

Title

One-Pot Synthesis of Copper Sulfide Nanowires/Reduced Graphene Oxide Nanocomposites with Excellent Lithium-Storage Properties as Anode Materials for Lithium-Ion Batteries

Permalink

Journal

ISSN

Authors

Feng, Caihong
Zhang, Le
Yang, Menghuan
et al.

Publication Date

DOI

Peer reviewed

One-pot synthesis of Copper sulfide nanowires /reduced graphene oxide nanocomposites with excellent lithium-storage properties as anode materials for lithium ion batteries.

Caihong Feng,[a,b]*Le Zhang,*[a] *Menghuan Yang,*[a] *Xiangyun Song*[b]*, Hui Zhao*[b] *,Zhe Jia*[b] *, Kening Sun**[a] *and Gao Liu**[b]

[a] School of Chemical Engineering and Environment, Beijing Institute of Technology, Beijing, 100081, P. R. China. Fax: +86 10 68912185; Tel: +86 10 68918696; E-mail: bitkeningsun@163.com

[b] Lawrence Berkeley National Laboratory 1 Cyclotron Rd., MS 70R108B, Berkeley, CA 94720, USA. Fax: 00 510 4867207 ; Tel: +1 510 486 7207 ; E-mail: gliu@lbl.gov

ABSTRACT: Copper sulfide nanowires/reduced graphene oxide (CuSNWs/rGO) nanocompsites are successfully synthesized via a facile one-pot and template-free solution method in a dimethyl sulfoxide (DMSO) – ethylene glycol (EG) mixed solvent. It is noteworthy that the precursor plays a crucial role in the formation of the nanocomposites structure. SEM, TEM, XRD, IR and Raman spectroscopy are used to investigate the morphological and structural evolution of CuSNWs/rGO nanocomposites. The as-fabricated CuSNWs/rGO nanocompsites show remarkably improved Li-storage performance, excellent cycling stability as well as high-rate capability compared with the pristine CuS nanowires. It obtains a reversible capacity of 620 mA

h g^{-1} at 0.5C after 100 cycles and 320 mA h g^{-1} at a high current rate of 4C even after 430 cycles. The excellent lithium storage performance is ascribed to the synergistic effect between CuS nanowires and rGO nanosheets. The as-formed CuSNWs/rGO nanocomposites can effectively accommodate large volume changes, supply a 2D conducting network and trap the polysulfides generated during the conversion reaction of CuS.

KEYWORDS: Copper sulfide, reduced oxide graphene, nanocomposites, lithium ion battery, synergistic effect.

1. INTRODUCTION

The increasingly emerging energy and environmental issues have constantly inspired enormous amount of research interest in advanced energy conversion and storage (ECS) devices.[1-3] The performance of these devices depends intimately on the properties of their materials, so it is critical to find innovative materials with new properties or routine ECS materials to meet the improving requirement for clean, efficient and sustainable energy supply.[4-5] Metal chalcogenides (MCs) are attracting significant attention due to their various applications in ECS devices including photocatalytic material, photothermal material, solar cells, electrocatalysis, Li-ion batteries (LIBs) and supercapacitors.[6-10]

Copper sulfides (Cu$_x$S) including CuS, Cu$_{1.96}$S, Cu$_{1.8}$S and Cu$_2$S are useful materials for energy storage applications due to its cost effectiveness and abundance in nature.[11-13] CuS has been used as electrode materials in LIBs owing to its good electrical conductivity (10^3 S cm^{-1}), high theoretical capacity (560 mA h g^{-1}) and flat discharge curves.[14-15] However, like most metal sulfide, it has some major drawbacks, including capacity fading and poor cyclability, which are associated with the pulverization of electrodes leading to the decay of the specific capacity and formation of polysulfides Li$_2$S$_x$ (2<x<8).[14,16-17] The polysulfides, the intermediates of the electrochemical reactions, can easily dissolve into organic electrolyte and migrate to the anode

2

side, leading to the poor capacity retention of LIBs. To deal with these issues, CuS micro-/nanostructure with different morphologies have been extensively investigated to improve their electrochemical properties by creating short diffusion lengths for Li^+ ions and increasing flexibility towards volume caused by Li^+ insertion/extraction. For example, Cai *et al*.[12] synthesized Cu_xS/Cu nanotubes and found that the nanotubes electrode present high discharge capacity of 526 mA h g^{-1} at a current density of 200 mA g^{-1} and good rate capability (282 mA h g^{-1} at 5 A g^{-1}). Zhang group[18] synthesized ultrathin CuS nanosheets which exhibit a large capacity, good cycling stability, and the capacity sustains at 642 mA h g^{-1} after 360 cycles at a current rate of 0.2 A g^{-1}. In addition, many researchers have to limit the potential window and sacrifice capacity to avoid lithium polysulfides dissolution.[14,19,20] Recently, studies showed that capping the sulfur or metal sulfide with thin graphene or graphene oxide layer could effectively reduce the dissolution of Li_2S_x into the electrolyte, and led to high reversible capacities and good rate capabilities.[21-23] This could be a promising strategy for the copper sulfide used as high performance electrode in LIBs by wrapping CuS nanocraystal with graphene to get high electrical conductivity, effective accommodation of the strain during Li^+ insertion/extraction and reduce polysulfides dissolution into the electrolyte during the repeated charging and discharging as well. Very recently, Tao *et al*.[24] have reported synthesis of the CuS/graphene composite as anode materials for LIBs and the obtained CuS/graphene composite exhibits a relatively high reversible capacity and good cycling stability. Ren and co-workers also reported double-sandwiched-like CuS/rGO structure for LIBs anode materials with enhanced electrochemical properties.[25] But there still exit challenge to meet the demanding requirements for LIBs with high charging/discharging rate, high capacity and long cycle life. One-dimensional CuS nanowires attract wide interest as electrode for LIBs due to their advantages in electronic conduction along the axial direction.[15,19] Encouraged by this, the design and fabrication of CuS nanowires/graphene (CuSNWs/rGO) composite could be a promising solution for high-performance LIB electrode materials. To the best of our knowledge, there is no report on the synthesis and electrochemical properties of CuS nanowires/graphene composite previously.

Herein, we develop a facile, one-pot approach to prepare CuSNWs/rGO nanocomposites by mixed solvent of dimethyl sulfoxide (DMSO) and ethylene glycol (EG). Comparing with other methods, [25-28] we successfully synthesized the nanocomposites without any surfactants or additional reductant. The rGO nanosheets act as conductive, elastically strong and electrochemically active substrate to produce the CuSNWs/rGO nanocomposites as anode materials. More importantly, the nanocomposites could facilitate the polysulfides dissolution. With the synergistic effect of CuS nanowires and rGO nanosheets, the as-produced CuSNWs/rGO nanocomposites are promising for application as high-rate LIBs electrode materials.

2. EXPERIMENTAL SECTION

2.1 Materials.

Thiourea (AR, 99.0%), copper (II) nitrate trihydrate ($Cu(NO_3)_2 \cdot 3H_2O$, AR, 99.5%), ethylene glycol (EG, AR) and dimethyl sulfoxide (DMSO, AR) were purchased from Beijing Chemical Company. Lithium-ion electrolytes were purchased from Zhangjiagang Guotai-Huarong New Chemical Materials Co., including 1 M $LiPF_6$ in ethylene carbonate (EC), diethyl carbonate (DEC) and dimethyl carbonate (DMC) with a volume ratio of 1:1:1. All chemicals were used without further purification.

2.2 Synthesis of the CuSNWs/rGO nanocomposites.

Graphene oxide (GO) was prepared from natural graphite powder via a modified Hummers method.[29] In a typical process, 46 mg of GO was dispersed in 90 mL of ethylene glycol (EG) by ultrasonic treatment for 2 h and then centrifuged at 4000 r/min for 20 min to remove undissolved large particles. The suspension was added to a three-necked flask with 30 mL of DMSO and 0.484 g of $Cu(NO_3)_2 \cdot 3H_2O$ (2 mmol) under magnetic stirring. Then, the flask was placed into oil bath and heated at 145°C for 6 h under nitrogen atmosphere. Finally, 10 mL of mixed solution containing 0.456 g (6 mmol) of thiourea was added to the solution drop by drop through a syringe under vigorous stirring and reacted for another 1.5 h. The final products were centrifuged

and washed several times by distilled water and ethanol, and finally freeze-dried for 48 h for further characterization.

For comparison, pristine CuS nanowires were prepared by a similar process in the absence of graphene oxide and bare rGO were synthesized in the same process except without addition of $Cu(NO_3)_2 \cdot 3H_2O$.

2.3 Material characterization.

The phase composition of the as-prepared samples were characterized by a Philips X'Pert Pro Multipurpose X-ray diffractometer (XRD) using Cu K_α radiation at 45 kV and 40 mA, at the 2θ range of 5-80° with 0.02 per step. The Raman spectra of the sample were collected using a Renishaw spectrophotometer equipped with a microscope having laser wavelength of 532 nm. The morphology of the samples and electrodes was characterized with a Quanta FEG 250 (FEI) field emission scanning electron microscope (SEM) system. High resolution transmission electron microscope (HRTEM) images were obtained on a JEOL JEM-2100F field emission microscope operated at 200 kV. X-ray photoelectron spectroscopy (XPS) was carried out on Physical Electronics 5400 ESCA. Fourier transform infrared (FT-IR) spectroscopy analysis was carried out in the range of 400-4000 cm^{-1} using a Nicolet iS10 (Thermo Scientific) spectrometer. TG/DTA analysis were performed with a TG/DTA 6200 (Seiko) apparatus at a heating rate of 10 °C min^{-1} in a flowing air to determine the amount of rGO in the samples.

Electrochemical measurement.

The coin-type cell were assembled in an argon-filled glove box. The working electrode was composed of 75wt% active material (CuSNWs/rGO nanocomposites), 10 wt% super P, 12 wt% carboxymethyl cellulose (CMC), and 3 wt% polyvinyl alcohol (PVA) dissolved in water. Lithium foil was used as the counter and reference electrode, and polypropylene membrane (Celgard 2400) as separator. The electrolyte solution was 1 M $LiPF_6$ dissolved in a mixture of ethylene carbonate (EC)/diethyl carbonate (DEC)/ dimethyl carbonate (DMC) (1:1:1 in volume). The galvanostatic charge/discharge measurements were performed using a Land Battery Measurement System (Wuhan, China) at various current densities of 0.1C-5C (1C = 560 mA h g^{-1})

with a voltage window of 0.02-3.00 V vs Li/Li^{+}. The cyclic voltammetry (CV) curves of materials were carried out by using CHI660D (Shanghai Chenhua Instrument) at a scanning rate of 0.1mVs[-1] between 0.02-3.00 V and electrochemical impedance spectroscopy (EIS) in the range of 10 mHz to 100 kHz on PARSTAT 2273. All the performances were tested at room temperature.

3. RESULTS AND DISCUSSION.

3.1 Characterizations of morphology and structure.

The XRD patterns of CuS nanowires, CuSNWs/rGO and GO are shown in Figure 1. All the diffraction peaks in Figure.1a can be indexed to the hexagonal phase of CuS (JCPDS No. 06-0464) and no impurity phases can be detected, indicating the formation of pure CuS and that they are highly crystallized. As shown in Figure.1b, the as-prepared GO after chemical oxidation exhibits a strong and sharp peak at 11.6°, which corresponds to the (002) interplanar spacing of 0.82 nm, indicating that the original Sp^2-bond carbon of graphite suffers breaking by oxidization.[26] For the CuSNWs/rGO composites (Figure.1c.), the characteristic peak of GO disappears due to the considerable reduction capability of EG, DMSO and thiourea at high temperature.[24,28,30] However, the characteristic stacking peak of rGO nanosheets at around 26° can not be identified from the XRD pattern of CuSNWs/rGO nanocomposites due to its low amount and low diffraction intensity.[24] From the TG analysis of CuSNWs/rGO nanocomposites (Supporting Information, Figure S1), the content of CuS in the composites is about 82.40 wt%. Besides, the broad diffraction peaks of CuS in CuSNWs/rGO composite indicated that the products have small sizes.[21]
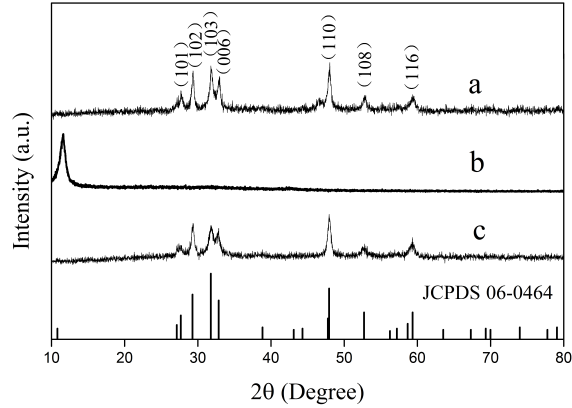
Figure 1. XRD patterns of (a) CuS nanowires, (b) GO, and (c) CuSNWs/rGO nanocomposites.

The reduction of the GO was also confirmed by Raman spectra. As shown in Figure 2a, both spectra exhibit two characteristic main peaks: the D band at $\sim$ 1357 cm[1] attributes to defects and disorder in the hexagonal graphitic layers and the G band at $\sim$ 1575 cm[1] corresponds to the vibration of sp^2 carbon atoms in a 2D hexagonal lattice.[26-28] It is found that the ratio value of I_D/I_G for CuSNWs/rGO nanocomposites and rGO is 1.14 and 1.07, respectively, which is higher than that of GO (0.86). The increased I_D/I_G is attributed to the decrease of the average size of sp^2 domains and the increased number of these domains, giving evidence that the GO was successfully reduced to form graphene.[26] Moreover, the strong and sharp band at $\sim$ 475 cm[1] in the spectra of CuSNWs/rGO nanocomposites agrees well with the observation for the covellite structure of CuS with a hexagonal crystal structure by previous references.[25, 27-28] The Raman results well agree with the XRD data.

7
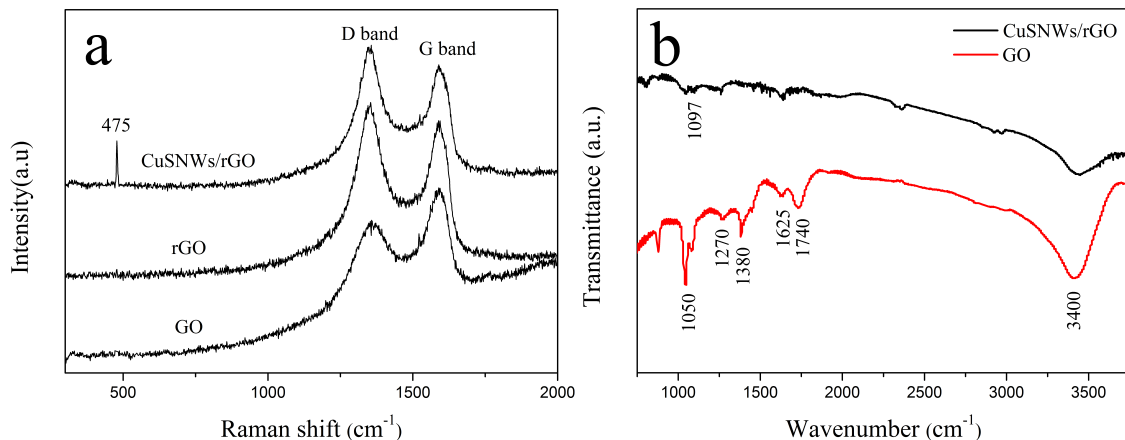
Figure 2. (a) Raman spectra of CuSNWs/rGO nanocomposites, rGO, and GO. (b) FT-IR spectra of GO and CuSNWs/rGO nanocomposites.

The prepared CuSNWs/rGO composites and pristine GO were further investigated by FTIR measurement. As shown in Figure 2b, the strong and broad band at around 3400 cm^{-1} is assigned to the stretching vibration of structural O-H and adsorbed water molecules.[30] The characteristic peak of the C=O stretching vibration appears at 1740 cm^{-1}.[28] Moreover, peaks at 1380, 1270 and 1050 cm^{-1} are observed in the spectrum of GO, which can be indexed to the stretching vibrations of C-OH, C-O-C and C-O, respectively.[30] However, most of these oxygen functional groups derived disappear in the spectrum of the CuSNWs/rGO composites, indicating that GO has been reduced to rGO. This agrees well with the XRD result and further confirms the formation of CuSNWs/rGO nanocomposites through this simple, one-pot method. Besides, the peaks of C-S stretching (1097 cm^{-1}) can be found in the spectrum of the CuSNWs/rGO composites indicating that CuS nanowires are chemically bonded to the rGO,[30] and these chemical bonds are important to the stability and electrochemical performance of the CuSNWs/rGO nanocomposites.
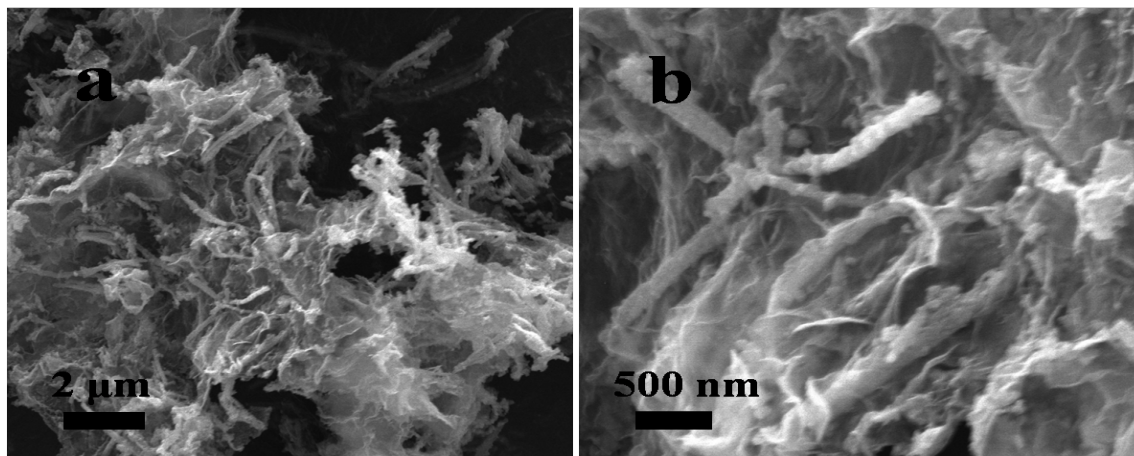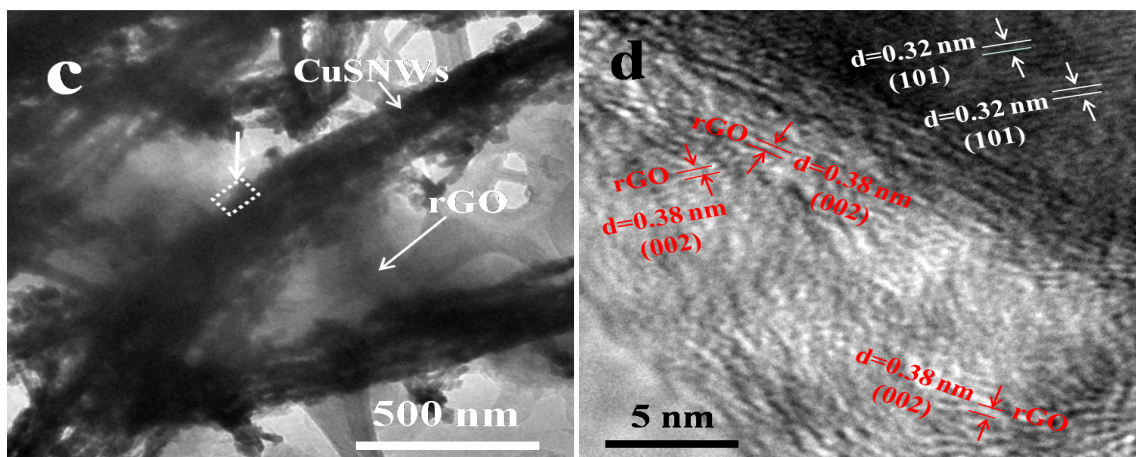
Figure 3. The SEM images of CuSNWs/rGO nanocomposites (a) low-magnification and (b) high-magnification. TEM images of CuSNW/rGO (c) and HRTEM image of CuSNWs/RGO nanocomposites (d).

   SEM and TEM were used to characterize the morphologies of the as-prepared CuSNWs/rGO nanocomposites. As shown in Figure 3a and Figure 3b, the CuS nanowires have rough surfaces and are wrapped by rGO nanosheets. Compared with the pristine CuS nanowires (Supporting Information, Figure S2a-2b), the nanowires are evenly distributed and the length become shorter than that of pristine CuS nanowires. It is suggested that rGO nanosheets may restrict CuS growth and aggregation.[31-32] More details of CuSNWs/rGO nanocomposite were further investigated by TEM and HRTEM and shown in Figure 3c and Figure3d. From the TEM we can clearly see that CuS nanowires are coated by rGO film and these nanowires are self-assembled into bundles. The HRTEM image (Figure 3d) of CuSNWs/rGO (indicated by dash line in Figure 3c) shows two kinds lattice fringes. One is semiordered with distance (d-spacing) of around 0.38 nm, corresponding to the d-spacing of rGO,[24, 33] and the other is ordered with fringe spaces of 0.32 nm, which can be indexed as the (101) planes of hexagonal CuS. All the above structural and morphological characterization confirms that CuSNWs/rGO nanocomposites can be well achieved by this simple and easily controlled approach.

To further understand the formation process of CuSNWs/rGO nanocomposites, control experiments were performed to understand the influence of thiourea. The intermediate in the

absent of thiourea and the product adding thiourea at the beginning of reaction were studied. As seen in Figure 4a, in the absent of thiourea, the resulted intermediate nanowires show tens of microns in length and smoother surface. However, when adding thiourea, $Cu(NO_3)_2 \cdot 3H_2O$ and solvent together at the beginning, the morphology of the product is CuS microsphere instead of nanowires dispersed in the rGO nanosheets (Figure 4b.). XRD pattern of the intermediate (Figure 4c) shows a strong peak appearing in the 10.44°, which is a striking similarity to those of other metal alkoxide precursors reported in the literature.[34-35] Since DMSO can interact with metal anions to form $M(DMSO)_x^+$ and M-DMSO complex,[36-37] the peak at 941cm^{-1} in the FT-IR spectrum (Figure 4d) corresponds to the S=O stretching band in the Cu-DMSO complex.[37] To analyze the chemical composition of intermediate and identify the chemical status of Cu, S, O elements in samples, X-ray photoelectron spectroscopy (XPS) analysis was carried out. The wide-scan XPS spectrum (Supporting Information, Figure S3a) evidently shows the signals of Cu, S, C, and O elements. The high-resolution XPS spectra (Supporting Information, Figure S3b-S3d) analysis shows that the intermediate contains Cu^{2+}, S^{2-} and C-O-R. Based on all these results, we infer that the intermediate should be a complex of $Cu(DMSO)_n(OCH_2CH_2O)/rGO$ and $Cu(DMSO)_nS/rGO$. Besides, the intermediate is vital to the ultimate morphology of CuS nanowire. It may act as a soft template and convert to final product CuSNWs/rGO nanocomposites after adding thiourea.The formation process of the CuSNWs/rGO nanocomposites is presented in scheme 1. First, Cu^{2+} cations favorably bind with oxygen-containing groups on GO sheets via the electrostatic interactions. If thiourea was added at the beginning, it reacts with Cu^{2+} immediately and only CuS microsphere coated by rGO nanosheets are obtained (scheme.1b). If thiourea was added after the formation of precursor, CuS nanowires wrapped by rGO nanocomposites are synthesized, as shown in scheme.1a.
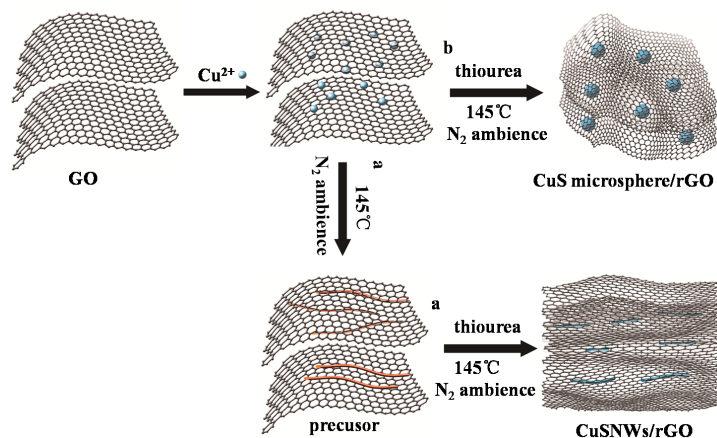
Scheme 1. Illustration of the formation process of CuSNWs/rGO nanocomposites.
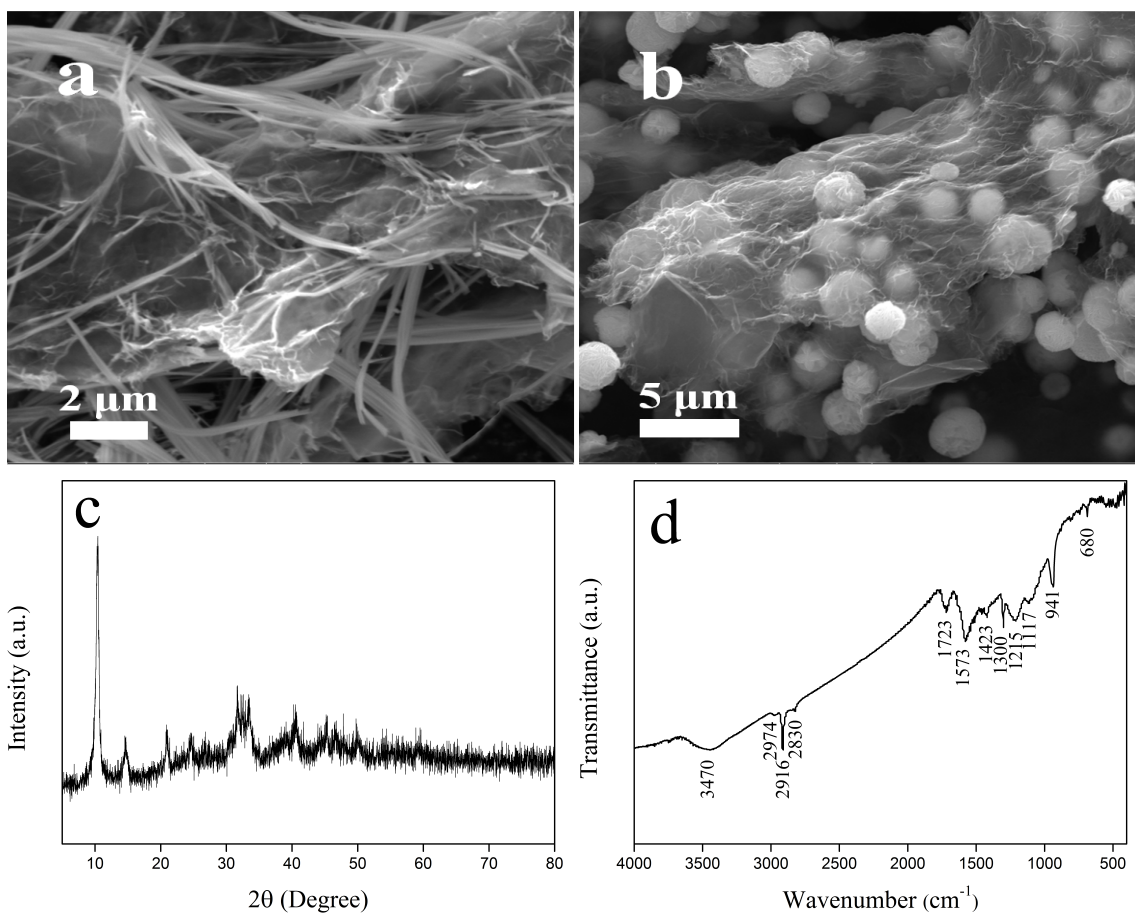
Figure 4. SEM image of intermediate (a), and CuS microshere/rGO composites (b). The XRD pattern of intermediate (c). The FT-IR spectra of intermediate (d).

3.2 Electrochemical performance.

The electrochemical properties of the CuSNWs/rGO nanocomposites for reversible Li+ storage

were investigated by electrochemical measurements. The results are shown in Figure 5.

The cyclic voltammogram of CuSNWs/rGO nanocomposites is given in Figure 5a, which elaborates the oxidation and reduction reactions due to the insertion and extraction of Li^{+} into electrode. In the first cycle, two reduction peaks are observed at around 1.6 and 2.0 V, and two oxidation peaks at around 1.9 and 2.4 V. In the subsequent cycles, one of the main cathodic peaks at 2.0 V shifts towards the higher potentials of 2.1 V and similarly the anodic peaks shift slightly negatively. The shift of the main cathodic peak towards a higher potential in the following cycles corresponds to a multi-step electrochemical reaction of lithium with the electrode that leads to the formation of a SEI film on the surface of the electrode, decomposition of the electrolyte, and the formation of Li_2S.[21, 25] So the two-step reaction of composite is elucidated by the following equations.

$$CuS + x\ Li^+ + x\ e^- \Longleftrightarrow Li_xCuS \qquad (1)$$

$$Li_xCuS + (2-x)\ Li^+ + (2-x)\ e^- \Longleftrightarrow Li_2S + Cu \qquad (2)$$
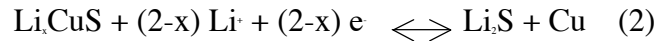
The transformation from CuS to LixCuS is related to the cathodic peak at 2.0 V, while that from LixCuS to Cu is associated with the cathodic peak at 1.6 V.[14-15, 24]
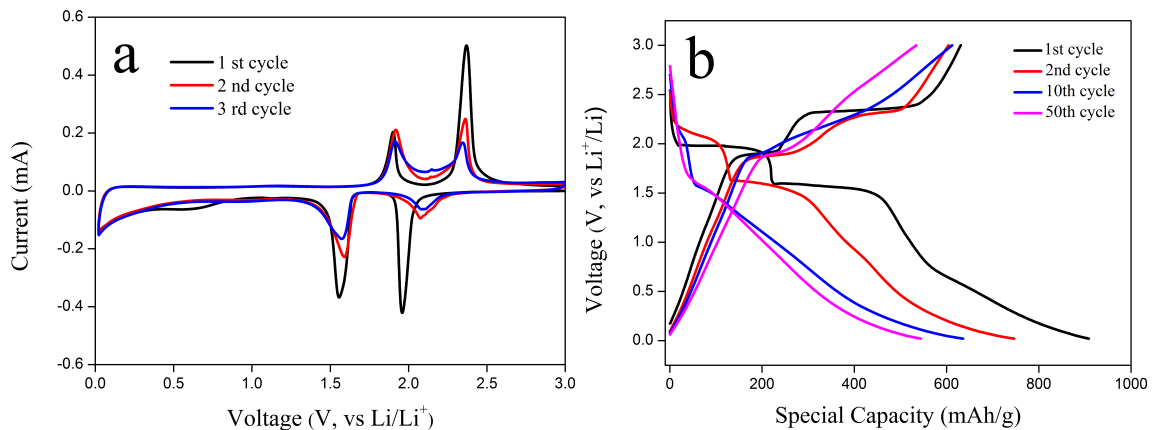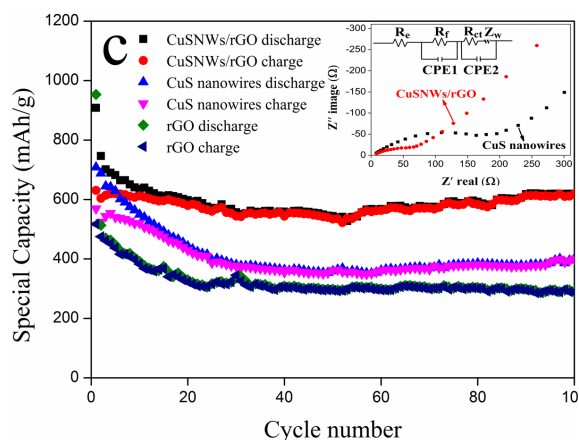
Figure 5. (a) CV response of the CuSNWs/rGO nanocomposites electrode. (b) Charge and discharge curves for the CuSNWs/rGO nanocomposites electrode at a rate of 0.5C between 0.02-3.00V. (c) Cycling performance of the CuSNWs/rGO nanocomposites electrode, CuS nanowires electrode, and rGO electrode at a current density of 0.5C within a voltage window of 0.02-3.00V. Inset: nyquist plots of CuSNWs/rGO nanocomposites electrode and CuS nanowires electrode after charge and discharge at 0.5C for 100 cycles and equivalent circuit model of the studied system.

Figure 5b illustrates the charge-discharge voltage profiles of the CuSNWs/rGO nanocomposites electrode for the first, second, tenth and fiftieth cycle at a constant current rate of 0.5 C. As shown in Figure 5b, two potential plateaus at around 2.0 V and 1.6 V observed in the initial charge process and two potential plateaus at around 1.9 V and 2.4 V observed in initial discharge process corresponds to the lithiation and delithiation of CuS electrode respectively, which are correlated with the discharge and charge plateaus in Figure 5a. For CuSNWs/rGO nanocomposites electrode, the potential plateaus of initial charge and charge curves agree well with that of CuS nanowires electrode (Supporting Information, Figure S4) except a plateau at around 0.7 V in the first discharge process (Figure 5b). It is well known that the plateau at about 0.7 V at the initial discharge process for carbon materials is generally ascribed to the formation of SEI film.[39] So the flat voltage at around 0.7 V should be related to the formation of solid electrolyte interface (SEI) film on the rGO surface. The initial discharge and charge capacities of CuSNWs/rGO electrode in the first cycle are 908 mA h g^{-1} and 630 mA h g^{-1}, respectively, based

13

on the whole weight of the composite. The large initial discharge capacity of CuSNWs/rGO nanocomposites may be attributed to the SEI layer on the surface of the elecreode due to electrolyte decomposition,[15,24,25] reduction of residual oxygen-containing groups on graphene and the irreversible reaction between Li and CuS as indicated in the equation (1) and (2).[40,41] The decrease in the area of the next cycle is consistent with the charge and discharge curves (Figure 5b), reflecting the capacity fading in subsequent cycles. It should be pointed out that the columbic efficiencies increase to almost unity at successive cycles, indicating that the formation of SEI during the first cycle is favourable and stable.[42]

The cycling performances of CuSNWs/rGO nanocomposites electrode comparing with bare CuS nanowires electrode and rGO nanosheets electrode at a current of 0.5 C are shown in Figure 5c. It is observed that the initial discharge capacity is 908, 708 and 953 mA h g^{-1} for CuSNWs/rGO nanocomposites, CuS nanowires and rGO nanosheets, respectively. The high initial discharge capacities are attributed to the formation of SEI film. After a few cycles, the CuS electrode shows a significant capacity decrease, while the intensity of capacity decreasing for CuSNWs/rGO is obviously smaller. This may attribute to the introduction of rGO nanosheets, which restricts the diffusion of polysulfides to some extent.[23] The CuS nanowires were wrapped by rGO nanosheets and evenly distributed in them, which can efficiently trap the polysulphides and suppress the outward diffusion. After 100 cycles the capacity of CuSNWs/rGO maintains at 620 mA h g^{-1}, and for CuS nanowires and rGO electrode the capacity keeps at 400 and 300 mA h g^{-1}, respectively. It is obvious to see that the composites have higher capacity than each individual component. Although various CuS and CuS/graphene as electrode material for LIBs have been studied, for example, Ma group have prepared a hybrid network CuS monolith cathode with a capacity of 468.3 mA h g^{-1} after 100 cycles (0.2 C, 1.0-3.0 V).[43] Wang et al. synthesised CuS cathode with a reversible capacity around 390 mA h g^{-1} after 100 cycles (0.5 C,1.2-3.0 V).[14] Ren and co-workers have fabricated "Double-Sandwich-Like" CuS@rGO as anode material, showing a capacity of 412.5 mA h g^{-1} at 0.5 C (0.001-3.00 V).[25] Tao *et al*. synthesized CuS/graphene composite exhibiting a capacity of 296 mAh g^{-1} after 25 cycles (50 mA g^{-1}, 0.01-3.0 V).[24] To our

knowledge, this large reversible capacity of CuS/rGO at 0.5C has not been witnessed in previous reports. The higher capacity and cycling stability can be attributed to the synergistic effect between CuS nanowires and rGO nanosheets as reported in the metal oxides/graphene composite and metal sulfide/graphene composite.[39, 42, 44-45] First, the unique structure contributes to the excellent electrochemical performance. On the one hand, the evenly distributed CuS nanowires could prevent rGO nanosheets from restacking, which can bring additional capacity from double-layer capacitance effect of rGO.[33] The capacitance effect was also suggested for enhanced Li-ion storage capacity in the graphene-based electrodes.[31,39] On the other hand, the introduction of rGO nanosheets can bind CuS nanowires and prevent these nanowires from aggregation, which can make fully contact with electrolyte and shorten the diffusion path of Li^+. Second, the conductivity of composite would be dramatically enhanced due to the presence of rGO nanosheets. Therefore, the electronic transport path way would be significantly shortened compared to pure CuS nanowires, leading to reduced particle-particle interface resistance.[46] Third, due to their porous and highly elastic nature, rGO nanosheets can effectively alleviate physical strains and absorb polysulfide anions.[44] Hence, the issue of the pulverization of the electrode material is greatly alleviated, and the cycle stable is remarkly improved. Here, it can be find that the capacity of CuSNWs/rGO nanocomposites decreased to 530 mA h g^{-1} and then increased to 620 mA h g^{-1}, indicating a possible activation process of electrode material.[18, 25]
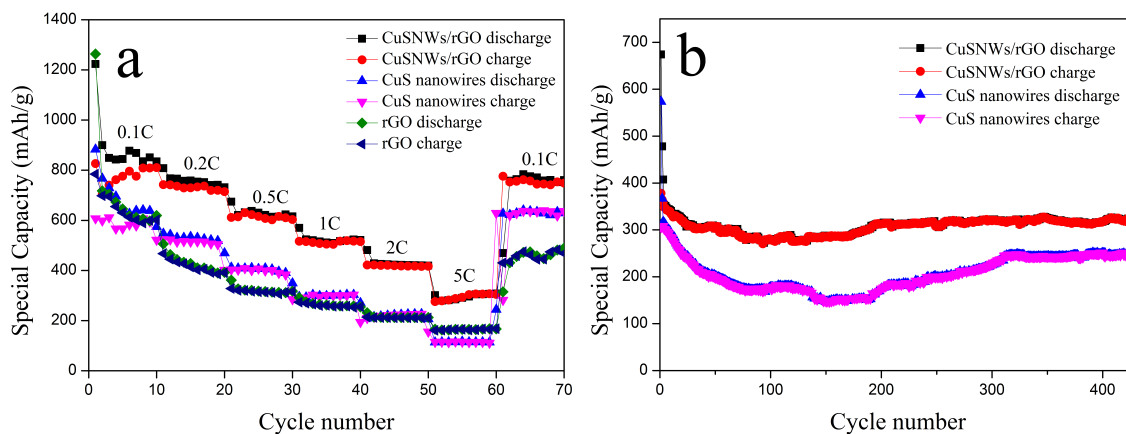
Figure 6. (a) Cycling performance of the CuSNWs/rGO nanocomposites electrode, CuS nanowires electrode, and rGO electrode at various current densities. (b) Cycling performance of the CuSNWs/rGO nanocomposites electrode and CuS nanowires electrode at 4C.

The high reversible capacity and excellent cycling behavior of the CuSNWs/rGO nanocomposites electrode is also exhibited in the rate capability. As shown in Figure 6a, at the maximum discharge rates studied 5 C (2.8 A g^{-1}), the material delivers a capacity of 300 mAh g^{-1}, higher than 115, 165 mA h g^{-1} for CuS nanowires and rGO. Additionally, the extraordinary cycling stability of the CuSNWs/rGO electrode is exhibited at various current densities. When the charge/discharge current density changes from 5 C to 0.1 C, the specific capacities of the composites return to 752 mA h g^{-1}, which do not ultimately change in the subsequent cycles, indicating extraordinarily high cycling stabilities. The excellent rate capability is also testified in Figure 6b. At the current density of 4 C, the capacity keeps stable and retains at 320 mA h g^{-1} even after 430 cycles, while the specific capacities of CuS nanowires is only 240 mA h g^{-1} and the stability is poor. The outstanding rate capability may be ascribed to two main aspects: (i) graphene acts as an elastic buffer and thereby accommodates volume expansion and shrinkage changes during the fast uptake and release of Li^+ at the high current; (ii) the superior conductivity of graphene enhances kinetics of the charge carrier transport.[40]

In order to get better understanding of the superior electrochemical performance of CuSNWs/rGO nanocomposites electrode compared to that of CuS nanowires electrode, electrochemical impedance spectroscopy (EIS) measurements were performed (inset in Figure 5c). The Nyquist plots are composed of a depressed semicircle in the high-to-medium frequency region and a sloping line in the low-frequency region. The depressed semicircle consists of two partly overlapped semicircles. The plots are fitted by an equivalent circuit.[33,40,44] As shown in the inset, the high-frequency semicircle region corresponds to SEI layer resistance and dielectric relaxation capacitance (R_f and CPE1), and the semicircle in low-frequency region corresponds to the charge-transfer resistance R_{ct} and CPE2 of electrode/electrolyte interface. The inclined line is

related to the lithium-diffusion process. The fitting results show that R_f and R_{ct} of CuS nanowires are 28.3Ω and 112.9 Ω, respectively. While the R_f and R_{ct} of CuSNWs/rGO composites are only 9.3Ω and 38.6Ω, respectively. The result confirms that the incorporation of rGO nanosheets not only preserve the high conductivity of CuSNWs/rGO nanocomposites electrode but also significantly enhance rapid electron transfer during the electrochemical lithium insertion/extraction. Therefore, the CuSNWs/rGO nanocomposites electrode exhibits high reversible capacity, excellent cyclic stability, and high-rate capability.

4. CONCLUSIONS

In a summary, CuSNWs/rGO nanocomposites were successfully synthesized by a facile one-pot method. The CuS nanowires are highly dispersed and anchored or wrapped in the rGO nanosheets. The composites exhibit excellent lithium-ion storage. Compared with CuS electrode, it shows a significant higher capacity with a reversible capacity of 620 mAh g^{-1} at 0.5C after 100 cycles. Even at a high current density of 4C, the specific capacity of CuSNWs/rGO nanocomposites electrode keeps stable and remains at 320mAh g-1 after 500 cycles. The excellent lithium storage performance of the CuSNWs/rGO composites is mainly attributed to two aspects: (i) the CuSNWs/rGO nanocomposites can effectively accommodate large volume changes during the charge/discharge process; (ii) the presence of rGO nanosheets with superior electronic conductivity supply 2D conducting network and absorb or trap the polysulfides generated during the conversion reaction of CuS, which improves the cycling stability of the electrode.

ASSOCIATED CONTENT

Supporting Information

The TG analysis of CuSNWs/rGO nanocomposites; SEM images of CuS nanowires; XPS analysis of CuSNW/rGO intermediate; Charge and discharge curves for the CuS nanowires electrode. This material is available free of charge via the Internet at http://pubs.acs.org.

AUTHOR INFORMATION

Corresponding Author

* E-mail: bitkeningsun@163.com. (K. Sun)

* E-mail: gliu@lbl.gov.   (G. Liu)

Notes

The authors declare no competing financial interest.

REFERENCES

1.   Aricò, A. S.; Bruce, P.; Scrosati, B.; Tarascon, J. M. and Schalkwijk, W. V. Nanostructured materials for advanced energy conversion and storage devices. Nat. Mater. 2005, 4, 366-377.

2.   Liu, C.; Li, F.; Ma, L.-P. and Cheng, H.-M. Advanced Materials for Energy Storage. *Adv. Mater.* **2010**, *22*, E28-E62.

3.   Yoo, H. D.; Markevich, E.; Salitra, G.; Sharon, D. and Aurbach, D. On the challenge of developing advanced technologies for electrochemical energy storage and conversion. *Mater. Today* **2014**, *17*, 110-121.

4.   Gao, M.-R.; Xu, Y.-F.; Jiang, J. and Yu, S.-H. Nanostructured metal chalcogenides: synthesis, modification, and applications in energy conversion and storage devices. *Chem. Soc. Rev.* **2013**, *42*, 2986-3017.

5.   Balaya, P. Size effects and nanostructured materials for energy applications. *Energy Environ. Sci.* **2008**, *1*, 645-654.

6.   Lai, C.-H.; Lu, M.-Y. and Chen, L.-J. Metal sulfide nanostructures: synthesis, properties and applications in energy conversion and storage. *J. Mater. Chem.* **2012**, *22*, 19-30.

7.   Wang, H.; Feng, H. and Li, J. Graphene and Graphene-like Layered Transition Metal Dichalcogenides in Energy Conversion and Storage. *Small* **2014**, *10*, 2165-2181.

8.   Gao, M.-R.; Jiang, J. and Yu, S.-H. Solution-Based Synthesis and Design of Late Transition Metal Chalcogenide Materials for Oxygen Reduction Reaction (ORR). *Small* **2012**, *8*, 13-27.

9.   Ramasamy, K.; Malik, M. A.; Revaprasadu, N. and O'Brien, P. Routes to Nanostructured Inorganic Materials with Potential for Solar Energy Applications. *Chem. Mater.* **2013**, *25*, 3551-3569.

10.   Zhao, Y. and Burda, C. Development of plasmonic semiconductor nanomaterials with copper chalcogenides for a future with sustainable energy materials. *Energy Environ. Sci.* **2012**, *5*, 5564-5576.

11.   Dennler, G.; Chmielowski, R.; Jacob, S.; Capet, F.; Roussel, P.; Zastrow, S.; Nielsch, K.; Opahle, I. and Madsen, G. K. H. Are Binary Copper Sulfides/Selenides Really New and Promising Thermoelectric Materials?. *Adv. Energy Mater.* **2014**, *4*, 130581.

12.   Cai, R.; Chen, J.; Zhu, J.; Xu, C.; Zhang, W.; Zhang, C.; Shi, W.; Tan, H.; Yang, D.; Hng, H. H.; Lim, T. M. and Yan, Q. Synthesis of Cu_xS/Cu Nanotubes and Their Lithium Storage Properties. *J. Phys. Chem. C* **2012**, *116*, 12468-12474.

13.   Hsu, Y.-K.; Chen Y.-C.; Lin, Y.-G. Synthesis of copper sulfide nanowire arrays for high-performance supercapacitors. *Electrochim. Acta* **2014**, *139*, 401-407.

14.   Wang, Y.; Zhang, X.; Chen, P.; Liao, H.; Cheng, S. In situ preparation of CuS cathode with unique stability and high rate performance for lithium ion batteries. *Electrochim. Acta* **2012**, *80*, 264-268.

15.   Feng, C.; Zhang, L.; Wang, Z.; Song, X.; Sun, K.; Wu, F.; Liu, G. Synthesis of copper sulfide nanowire bundles in a mixed solvent as a cathode material for lithium-ion batteries. *J. Power Sources* **2014**, *269*, 550-555.

16.   Jache, B.; Mogwitz, B.; Klein, F.; Adelhelm, P. Copper sulfides for rechargeable lithium batteries: Linking cycling stability to electrolyte composition. *J. Power Sources* **2014**, *247*, 703-711.

17.   Han, F.; Li, W.-C.; Li, D. and Lu, A.-H. In Situ Electrochemical Generation of Mesostructured Cu_2S/C Composite for Enhanced Lithium Storage: Mechanism and Material Properties. *ChemElectroChem* **2014**, *1*, 733-740.

18.   Du, Y.; Yin, Z.; Zhu, J.; Huang, X.; Wu, X.-J.; Zeng, Z.; Yan, Q. and Zhang, H. A general method for the large-scale synthesis of uniform ultrathin metal sulphide nanocrystals. *Nat. Commun.* **2012**, *3*,1177.

19.   Zhang, B.; Gao, X.-W.; Wang, J.-Z.; Chou, S.-L.; Konstantinov, K.; and Liu, H.-K. CuS Nanoflakes, Microspheres, Microflowers, and Nanowires: Synthesis and Lithium Storage Properties. *J. Nanosci. Nanotechnol.* **2013**, *13*, 1309-1316.

20.   Chen, Y.; Davoisne, C.; Tarascon, J.-M. and Guéry, C. Growth of single-crystal copper sulfide thin films via electrodeposition in ionic liquid media for lithium ion batteries. *J. Mater. Chem.* **2012**, *22*, 5295-5299.

21.   Mahmood, N.; Zhang, C.; Jiang, J.; Liu, F. and Hou, Y. Multifunctional Co_3S_4/Graphene Composites for Lithium Ion Batteries and Oxygen Reduction Reaction. *Chem. Eur. J.* **2013**, *19*, 5183-5190.

22.   Ji, L.; Rao, M.; Zheng, H.; Zhang, L.; Li, Y.; Duan, W.; Guo, J.; Cairns, E. J. and Zhang, Y. Graphene Oxide as a Sulfur Immobilizer in High Performance Lithium/Sulfur Cells. *J. Am. Chem. Soc.* **2011**, *133*, 18522-18525.

23.   Zhao, M.-Q.; Zhang, Q.; Huang, J.-Q.; Tian, G.-L.; Nie, J.-Q.; Peng, H.-J. and Wei, F. Unstacked double-layer templated graphene for high-rate lithium-sulphur batteries. *Nat. Commun.* **2014**, *5*, 3410.

24.   Tao, H.-C.; Yang, X.-L.; Zhang, L.-L. and Ni, S.-B. One-pot facile synthesis of CuS/graphene composite as anode materials for lithium ion batteries. *J. Phys. Chem. Solids* **2014**, *75*, 1205-1209.

25.   Ren, Y.; Wei, H.; Yang, B.; Wang, J.; Ding, J. "Double-Sandwich-Like" CuS@reduced graphene oxide as an Anode in Lithium Ion Batteries with Enhanced Electrochemical Performance. *Electrochim. Acta* **2014**, *145*, 193-200.

26.   Xie, J.; Liu, S.; Cao, G.; Zhu,T.; Zhao, X. Bai, J. Self-assembly of CoS₂/graphene nanoarchitecture by a facile one-pot route and its improved electrochemical Li-storage properties. *Nano Energy*, 2013, 2, 49-56

27.   Zhang, Y.; Tian, J.; Li, H.; Wang, L.; Qin, X.; Asiri, A. M.; Al-Youbi, A. O. and Sun, X. Biomolecule-Assisted, Environmentally Friendly, One-Pot Synthesis of CuS/Reduced Graphene Oxide Nanocomposites with Enhanced Photocatalytic Performance. *Langmuir* **2012**, *28*, 12893-12900.

28.   Zhang, X.-J.; Wang, G.-S.; Wei, Y.-Z.; Guo, L. and Cao, M.-S. Polymer-composite with high dielectric constant and enhanced absorption properties based on graphene–CuS nanocomposites and polyvinylidene fluoride. *J. Mater. Chem. A* **2013**, *1*, 12115-12122.

29.   Hummers, W. S.; Offeman, R.E. Preparation of graphitic oxide, *J.Am.Chem. Soc.*, **1958**, 80, 1339-1339

30.   Wang, Y.; Zhang, L.; Jiu, H.; Li, N.; Sun, Y. Depositing of CuS nanocrystals upon the graphene scaffold and their photocatalytic activities. *Appl. Surf. Sci.* **2014**, *303*, 54-60.

31.   Gu, Y.; Xu, Y.; Wang, Y. Graphene-Wrapped CoS Nanoparticles for High-Capacity Lithium-Ion Storage. *ACS Appl. Mater. Interfaces* **2013**, *5*, 801-806.

32.   Sun, Y.; Hu, X.; Luo, W.; Xia, F. and Huang, Y. Reconstruction of Conformal Nanoscale MnO on Graphene as a High-Capacity and Long-Life Anode Material for Lithium Ion Batteries. *Adv. Funct. Mater.* **2013**, *23*, 2436-2444.

33.   Pan, Q.; Xie, J.; Liu, S.; Cao, G.; Zhu, T. and Zhao, X. Facile one-pot synthesis of ultrathin NiS nanosheets anchored on graphene and the improved electrochemical Li-storage properties. *RSC Adv*. **2013**, *3*, 3899-3906.

34.   Larcher, D.; Sudant, G.; Patrice, R. and Tarascon, J.-M. Some Insights on the Use of Polyols-Based Metal Alkoxides Powders as Precursors for Tailored Metal-Oxides Particles. *Chem*. *Mater*. **2003**, *15*, 3543-3551.

35.   Ma, X.-H.; Feng, X.-Y.; Song, C.; Zou, B.-K.; Ding, C.-X.; Yu, Y.; Chen, C.-H. Facile synthesis of flower-like and yarn-like   -Fe_2O_3 spherical clusters as anode materials for lithium-ion batteries. *Electrochim*. *Acta* **2013**, *93*, 131-136.

36.   Wankhede, M. E. and Haram, S. K. Synthesis and Characterization of Cd-DMSO Complex Capped CdS Nanoparticles. *Chem*. *Mater*. **2003**, *15*, 1296-1301.

37.   Stone, J. A.; Su, T. and Vukomanovic, D. A collisionally activated dissociation (CAD) and computational investigation of doubly and singly charged DMSO complexes of Cu^{2+}. *Can*. *J*. *Chem*. **2005**, *83*, 1921-1935.

38.   Cotton, F. A.; Francis, R. and Horrocks, W. D. Sulfoxides as ligands. Ⅱ. The infrared spectra of some dimethyl sulfoxide complexes. *J*. *Phys*. *Chem*. **1960**, *64*, 1534-1536.

39.   Guo, P.; Song, H.; Chen, X. Electrochemical performance of graphene nanosheets as anode material for lithium-ion batteries. *Electrochem*. *Commun*. **2009**, *11*, 1320-1324.

40.   Wang, Z.; Chen, T.; Chen, W.; Chang, K.; Ma, L.; Huang, G.; Chen, D. and Lee, J. Y. CTAB-assisted synthesis of single-layer MoS_2–graphene composites as anode materials of Li-ion batteries. *J*. *Mater*. *Chem*. *A* **2013**, *1*, 2202-2210.

41.   Xu, C.; Zeng, Y.; Rui, X.; Xiao, N.; Zhu, J.; Zhang, W.; Chen, J.; Liu, W.; Tan, H.; Hng, H. H. and Yan, Q. Controlled Soft-Template Synthesis of Ultrathin C@FeS Nanosheets with High-Li-Storage Performance. *ACS Nano* **2012**, *6*, 4713-4721.

42.   Huang, X.-L.; Wang, R.-Z.; Xu, D.; Wang, Z.-L.; Wang, H.-G.; Xu, J.-J.; Wu, Z.; Liu, Q.-C.; Zhang, Y; Zhang, X.-B. Homogeneous CoO on Graphene for Binder-Free and Ultralong-Life Lithium Ion Batteries. *Adv*. *Funct*. *Mater*. **2013**, *23*, 4345-4353.

43.   Cheng, J.; Pan, Y.; Zhu, J.; Li, Z.; Pan, J.; Ma, Z. Hybrid network CuS monolith cathode materials synthesized via facile in situ melt-diffusion for Li-ion batteries. *J. Power Sources* **2014**, *257*, 192-197.

44.   Mahmood, N.; Zhang, C. and Hou, Y. Nickel Sulfide/Nitrogen-Doped Graphene Composites: Phase-Controlled Synthesis and High Performance Anode Materials for Lithium Ion Batteries. *Small* **2013**, *9*, 1321-1328.

45.   Zhou, X.; Zhang, J.; Su, Q.; Shi, J.; Liu, Y.; Du, G. Nanoleaf-on-sheet CuO/graphene composites: Microwave-assisted assemble and excellent electrochemical performances for lithium ion batteries. *Electrochim. Acta* **2014**, *125*, 615-621.

46.   Nethravathi, C.; Rajamathi, C. R.; Rajamathi, M.; Wang, X.; Gautam, U. K.; Golberg, D. and Bando, Cobalt hydroxide/oxide hexagonal ring-graphene hybrids through chemical etching of metal hydroxide platelets by graphen oxide:energy storage applications.Y. *ACS Nano*, **2014**, *8*, 2755-2765.

Abstract Graphic

CuSNWs/rGO nanocomposites